Acta Oncologica 29 (1990) Fasc. 5

FROM THE DEPARTMENTS OF RADIATION PHYSICS AND ONCOLOGY, UNIVERSITY HOSPITAL, LUND, SWEDEN.

CALCULATION AND MEASUREMENTS OF ABSORBED DOSE IN TOTAL BODY IRRADIATION

G. SVAHN-TAPPER, P. NILSSON, C. JÖNSSON and T. A. ALVEGÅRD

Abstract

A method which is simple, reliable, and rapid to use in clinical routine for basic dose calculation in total body irradiation (TBI) has been tested with 8 MV x-rays. The dosimetry follows, as far as possible, national and international recommendations for conventional radiotherapy. The dose rate at different locations and depths is calculated from the absorbed dose rate at dose maximum for a phantom size of 30 × 30 × 30 cm in the TBI field ($\mathring{D}_c$), an inverse square law factor (SAD^2/SPD^2), the tissue-maximum ratio (TMR), an equivalent phantom and patient size correction factor (A), a factor for lack of back-scattering material (B), an off-axis output correction factor (O), and a factor that corrects for off-axis variations in effective photon beam energy and for oblique beam penetration of the patient (R). The collimator opening is constant for all patient sizes. It is shown that TMR, A, B and R can be measured in conventional geometry in ordinary phantoms but at an extended distance, while $\mathring{D}_c$, O and SAD^2/SPD^2 must be measured in TBI geometry. Tests in Humanoid phantoms showed an agreement in measured and planned AP/2 doses of 2% or better. If the calculation method is used for lower photon energies or in other TBI geometries it may be necessary to correct for the elliptical shape of the patient and for back-scattered radiation from the walls or floor.

Key words: Total body irradiation, bone marrow transplantation, dosimetry, radiotherapy, 8 MV x-rays, leukaemia

Chemotherapy and marrow grafting for patients with acute leukaemia who have failed chemotherapy, result in cure rates of 10%–30% (1). For patients under the age of 50 with acute non-lymphoblastic leukaemia transplanted in first remission, the cure rate is approximately 50%, with better results in younger patients (2). In most radiotherapeutic procedures there is a balance between cure and severe side effects. This is also valid when conditioning leukaemia patients with total body irradiation (TBI), especially concerning their lung tissue (3–5). General recommendations for dosimetry and measurement techniques in TBI-fields have been presented at the Leiden meeting (6) and by AAPM (7). Review articles with extensive literature references have been written e.g. by Glasgow (8) and Quast (9, 10).

To secure good dosimetric accuracy in the patient there is a need both for good fundamental dosimetry and for different compensation (filter) techniques to adjust for changes in body contours, body heterogeneities and variation of absorbed doses in different human tissues. Some kind of patient fixation is also necessary. Basic dosimetric measurements in TBI geometry are cumbersome due to the need for large phantoms, the use of 'primitive' treatment couches and the low dose rate combined with irradiation of detector cables. Thus, it is essential to investigate which dosimetric parameters can eventually be measured in conventional geometry in ordinary phantoms and which parameters must be measured in TBI geometry.

The aim of this work was to test a method of calculation which can be further developed to include, for example the construction of compensating filters. The methods used are as far as possible founded on national and international dose protocols for conventional dosimetry.

Material and Methods

Patient set-up and dose fractionation schedule. An 8 MV linear accelerator (Philips SL75/14), in a room designed for conventional radiation therapy, is used for the TBI. A schematic drawing of the treatment set-up is shown in Fig. 1. The field is used on the diagonal with a field size of 172 × 172 cm with rounded corners. The TBI couch has a perspex top, and a 10 mm thick perspex spoiler is fixed in front of the patient to eliminate the build-up region.

Accepted for publication 26 July 1989.

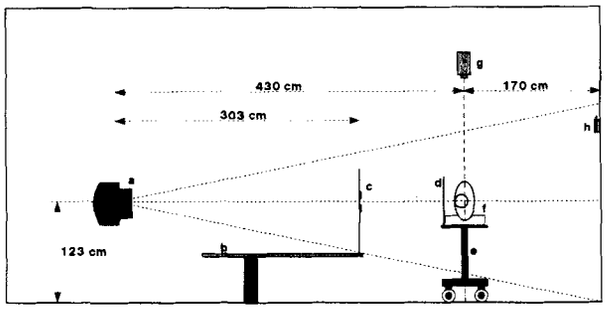

Fig. 1. Treatment set-up (a: Linac head, b: Ordinary treatment couch, c: Lung shielding blocks, d: Perspex spoiler, e: TBI couch, f: Patient in styrofoam cast, g: Laser, h: Ion chamber).

The patient is treated isocentrically with an AP-PA technique where the 'source-axis' distance (SAD = 430 cm) is defined by a laser line. Two individually designed casts of styrofoam are made, the patient lying on his left and right side respectively. Lung blocks are made of Rose's metal (25% Sn, 50% Bi, 25% Pb), one pair for each position of the patient. The blocks are placed 303 cm from the source and the position is verified by localization and verification films. Bolus ('superflab') is used in the head and neck region and on the top of the skull.

A total body dose of 12 Gy and a dose to the shielded lungs of 9.6 Gy is given in 6 fractions with two fractions per day separated in time by 8 h. The linac dose rate is 0.10 Gy/min while the mean dose rate is 2 Gy/35 min at the center of the patient at the level of the umbilicus.

Dosimetry. The dose rate at an arbitrary point is calculated as in conventional radiation therapy for an isocentric treatment but corrected for lack of back-scatter and off-axis effects. The field size in conventional radiation therapy is replaced with a factor representing phantom or patient size in the TBI geometry.

The dose rate, $\mathring{D}$, at an arbitrary point is calculated by the expression:

$$\mathring{D} = \mathring{D}_c \cdot (SAD/SPD)^2 \cdot TMR \cdot A \cdot B \cdot O \cdot R \qquad (1)$$

where:

$\mathring{D}_c$ = the dose rate at a depth of 2 cm and at an SAD of 430 cm for a reference phantom (30 × 30 × 30 cm) with the spoiler present,
SAD = source-axis distance (= 430 cm),
SPD = distance from source to point of interest,
TMR = tissue-maximum ratio for the equivalent phantom or patient size valid at the point of interest,
A = correction for equivalent phantom size normalized to the reference phantom,
B = correction for lack of back-scattering material,
O = correction for beam profile variations,
R = correction of TMR for off-axis effects.

Measurement procedures. In the measurements of depth doses and phantom-size dependence, water phantoms were placed with the frontal side at 430 cm from the source. Tissue-maximum ratios were calculated from the percentage depth doses (more convenient to measure than TMR) and normalized peak-scatter factors (NPSF) measured in conventional geometry according to the British Journal of Radiology, Supplement No. 17 (11). Since sector integration of patient silhouettes (12) shows a variation in 'equivalent squares' at different levels of $(30 \pm 20)^2$ cm, a 30 × 30 × 30 cm phantom was chosen as a reference phantom in the calculation and measurements, instead of the 10 × 10 cm reference field used in conventional radiation therapy. Dose calibration in the TBI field was made at an SSD of 428 cm and at a depth of 5 cm in the 30 × 30 × 30 cm water phantom with the spoiler positioned 15 cm in front of the phantom and with a 0.6 cm^3 BF-ionization chamber as detector. This calibration was also performed in a 30 × 30 × 30 cm polystyrene phantom with TLD (both chips and rods), calibrated with a ^{60}Co unit and corrected for energy dependence. For tests in Humanoid phantoms (Humanoid Systems, Carson, CA, USA) TLD-rods were used. Build-up measurements were made with a diode (Therados) in a large water phantom.

The attenuation coefficient for Rose's metal was determined in TBI geometry. To verify the lung doses, catheters were taped on the ventral and dorsal sides of the thorax.

A computer program for a PC was written for the calculation of absorbed dose rates at arbitrary points in phantoms or patients. The parameters TMR, A, B, O, and R are stored as matrixes and linear interpolation is performed for the input parameters of depth, equivalent phantom size and off-axis distance in the gun-target direction.

The calculation of absorbed doses at different levels in the Humanoid phantoms and patients are made from measurements of the AP-distances, the off-axis distances and the 'equivalent squares' based on the patient silhouette (Table).

Results and Discussion

Percentage depth dose and tissue-maximum ratios. Percentage depth doses measured both in a rectangular phantom with dimensions 20 × 63 cm (depth 60 cm) in the TBI field and in a 25 × 25 cm field defined by the collimators at a source–phantom distance of 430 cm agreed to within ±1% and were also equivalent to the depth dose of a 25 × 25 cm field measured at a source–phantom distance of 100 cm, and recalculated to 430 cm.

With the spoiler 15 cm in front of the phantom, the depth dose increased by 1% at 2 cm depth if the spoiler correction factor was determined at 5 cm depth. For larger depths the spoiler did not influence the depth dose. Other authors have also found an agreement between depth doses recalculated from conventional geometry and from TBI geometry (13, 14). This is only valid if the contribution from collimator scatter is negligible. This effect is largest for a short SSD (11).

Table

Input data and calculated AP/2 and skin absorbed doses for a ventral (F1) and a dorsal (F2) TBI field. The monitor units are calculated for an AP/2 dose of 2.0 Gy at the level of the umbilicus

Level	Eyes	Neck	Jugulum	Pr.xiph	Umbil.	Cent.ray	Thighs	Legs
AP ventral	10.2	8.0	6.2	10.2	9.0	9.0	12.0	5.5
AP dorsal	8.6	7.6	9.0	9.4	9.0	9.0	3.4	4.1
Off-axis dist	47.4	36.2	21.2	12.3	0.0	0.0	28.5	59.6
'Equiv size'	19.1	24.8	29.1	33.0	33.6	33.6	28.5	21.5
Abs. dose (Gy) for 2 Gy in mid-point dose at the level of the umbilicus:								
AP/2								
F1	0.99	1.04	1.04	1.00	1.00	1.00	1.07	1.10
F2	0.98	1.04	1.06	1.00	1.00	1.00	1.03	1.09
F1 + F2	1.97	2.09	2.10	2.00	2.00	2.00	2.10	2.19
Ventral								
F1	1.22	1.22	1.21	1.23	1.20	1.20	1.24	1.19
F2	0.70	0.80	0.83	0.72	0.74	0.74	0.80	0.93
F1 + F2	1.92	2.02	2.03	1.94	1.94	1.94	2.04	2.12
Dorsal								
F1	0.70	0.80	0.82	0.72	0.74	0.74	0.83	0.94
F2	1.21	1.22	1.22	1.22	1.20	1.20	1.19	1.18
F1 + F2	1.92	2.02	2.04	1.94	1.94	1.94	2.03	2.12

MONITOR UNITS/FIELD = 1950

Since central-axis depth doses can be measured in conventional geometry at the TBI distance and collimator scatter is almost independent of the position of the jaws for fields of the same dimensions (15), off axis depth doses were measured in a large water phantom in fields defined by the asymmetric jaws (Fig. 2). The measurements were made parallel to the central ray at 35 cm and at 70 cm off axis both on the gun side and on the target side of the accelerator. Fig. 2 shows the off-axis TMRs normalized to the TMR on the central beam for the 25 × 25 cm field. The differences between central TMR and TMR at 35 cm and at 70 cm off axis are 1% and 4–5% respectively for large depths. The same differences were found for a 35 × 35 cm field. These differences arise from the production of radiation with lower energy in distal parts of the beam compared with the central ray (16, 17).

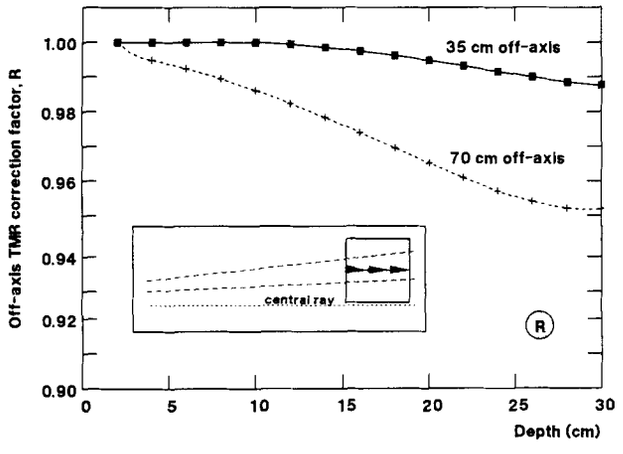

Fig. 2. Correction of TMR for off-axis effects, R, versus depth.

Thus in TBI, the central depth dose or TMR is not valid in the head and neck region and in the legs. The same effect was shown by Findley et al. (18) for TBI fields with 10 MV x-rays.

Phantom size dependence. Fig. 3 shows the variation in output as a function of equivalent phantom cross section without the spoiler, measured at 5 cm depth and recalculated to 2 cm depth. The results were normalized to the 30 × 30 × 30 cm water phantom. With the spoiler at 1.5 cm, 15 cm and 30 cm in front of the phantom, no significant difference was found compared to the measurements without the spoiler.

In TBI we always use fully opened diaphragms. This means that the amount of scattered radiation varies only with phantom size and can be described by the normalized peak-scatter factor, NPSF (11). The values were normalized to the 30-cm cubic phantom. Fig. 3 shows that the agreement between NPSF and phantom-scatter correction measured in the TBI geometry is excellent for phantom sizes larger than 20 × 20 × 30 cm, in agreement with the measurement by Podgorsak et al. (19). For smaller phantom sizes there is less attenuation of the back-scattered radiation from the wall. This is demonstrated by the phantom-size correction determined in the 10.2 × 20 × 30 cm phantom

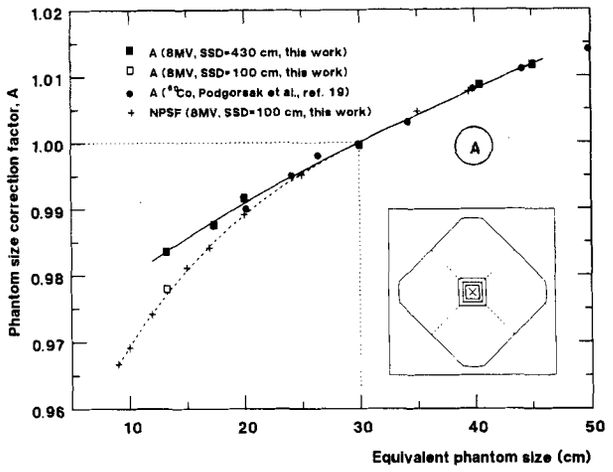

Fig. 3. Phantom size correction factor, A, versus side of equivalent phantom size at SSD = 430 cm (■) and at SSD = 100 cm (□). Normalized peak scatter factors (NPSF) measured at SSD = 100 (+) cm are also shown.

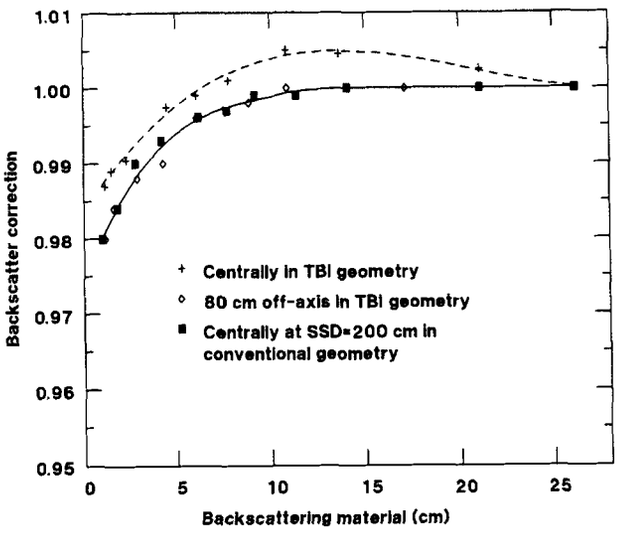

Fig. 4. The effect of lack of back-scattering material measured in different geometries.

placed with its back at 470 cm instead of at 140 cm from the wall, and normalized to the 30-cm cubic phantom at the same distance (open square in Fig. 3).

In Fig. 3 is also plotted the relative dose at d_{max} (corresponding to our parameter A) for large phantoms and ^{60}Co radiation measured by Podgorsak et al. (19). With a normalization for the phantom with the 30 × 30 cm cross section, NPSF is almost independent of photon energy from ^{60}Co to 10 MV (19) for phantom sizes corresponding to TBI.

The inverse square law. No systematic deviation from the inverse square law was found when it was tested at the center of the TBI-field with the ionization chamber at a depth of 2 cm and 28 cm in the 30 × 30 × 30 cm phantom for focus-phantom distances of 430 ± 25 cm.

Lack of back-scattering material. The effect of lack of back-scattering material was independent of the phantom depth in front of the ionization chamber when tested at depths of 8 cm, 13 cm, and 26 cm for different phantom cross sections. This is in agreement with the results of Van Dyk et al. (20) for ^{60}Co radiation. In the following experiments the ionization chamber was placed at a depth of 10 cm.

Fig. 4 shows a comparison of the effect of lack of back-scattering material for the 20 × 20 cm polystyrene phantom in the center of the TBI field, 80 cm off axis in the TBI field and in a field extending 2 cm outside the phantom at a focus-phantom distance of 200 cm. In the centre of the TBI field, the back-scattered radiation from the wall can be seen. This is not the case at 80 cm off axis. Since the effect of the back scatter from the wall can be seen only in central parts of the field, lack of phantom back scatter was measured far from the wall at a source-phantom distance of 200 cm with fields extending 2 cm outside the phantom. The results are shown in Fig. 5. The data were normalized to 25 cm of back-scattering material, in agreement with the conditions in the dose-calibration measurements and in the measurements of the phantom size dependence. A comparison of 20 cm of water and 20 cm of polystyrene as back-scattering material showed a complete equivalence between the two phantom materials.

The effect of the amount of back-scattering material has been studied before for ^{60}Co radiation, 2.5 MV, 4 MV, 6 MV and 10 MV x-rays (19–21). The effect diminishes with increasing photon energy.

From the test of the inverse square law, it can be concluded that the contribution from back-scattered photons is constant for distances of 170 ± 25 cm from the wall for a projected field size of about 5.5 m^2. Back scatter from

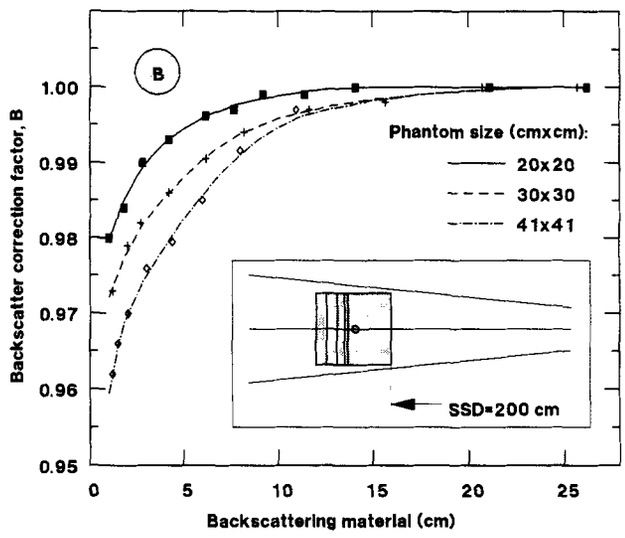

Fig. 5. Correction factor, B, for lack of back-scattering media normalized to 25 cm of back-scattering material.

the wall has also been noticed for ^{60}Co radiation (20, 22). If the patient is placed near a concrete wall this effect must be studied and taken into account.

Beam profiles in air. Five beam profiles in the gun-target direction measured free in air at a focus distance of 430 cm showed that the useful length of the field is 170 cm, with a variation of $\pm 3\%$ in the 'free in air' absorbed dose. The presence or absence of the spoiler produced no significant differences in the beam profiles.

The beam profile in air also includes back-scattered photons from the concrete wall. Fig. 4 shows that the albedo will influence the central parts of the TBI field, to which the normalization is made, but not the distal parts. The albedo is estimated to be 1% of the air dose in the centre of the field.

Dose calibration. The dose rate determined by the ionization chamber in the reference phantom is used in patient treatments. Since the corrections for stem and cable effects were as small as 0.4%–1.0% (23, 24) and of different signs they were neglected.

The relative dose rate determined by TLD chips and TLD rods in polystyrene differed by 0.1% and was 0.5% lower than the dose rate in water measured with the ionization chamber.

The determination of dose rate in the reference phantom in the TBI geometry is very crucial since errors in this measurement introduce a systematic error in the whole TBI dosimetry. In TBI the machine is operating over long irradiation times, which may influence the stability of the accelerator and the constancy of the monitor ionization chamber. It is thus essential to simulate the operating conditions used in TBI in the calibration procedure. The stem and cable of the ionization chamber are irradiated, resulting in effects that are difficult to evaluate (25). The determination of absorbed dose is also influenced by the difference in the spectra inside the 30-cm cubic phantom with fully opened diaphragms compared to the 10×10 cm field defined by the jaws. For that reason and because TLD is also used in the Humanoid phantoms and for dosimetry in vivo, we also used TLD rods and chips in a polystyrene phantom as a check of the dose calibration. The way the TLD was used eliminated both the individual sensitivity and the supralinearity correction and, according to ICRU 21 (26), there is no dose-rate effect in LiF. The difference in the spectra in the 30-cm cubic phantom and the 10×10 cm field introduces an uncertainty in the recalculation of the TLD signal to the absorbed dose in polystyrene because some sort of cavity theory must be used. According to Cunningham et al. (27), the ratios of average mass-energy absorption coefficients between water and polystyrene are also influenced by the differences in the spectra. Since the difference of 0.5% in dose rate determined with the ionization chamber and with TLD is fairly small and the probability of making the same systematic error with the two methods used is negligible, the value determined with the ionization chamber is used in the calculations according to conventional dose calibration methods.

Build-up measurements. The absorbed doses at a depth of 0.6 mm (the thickness of the phantom wall and the detector), which is approximately the depth of the superficial blood vessels, varied from 98 to 91% with a maximum of 103% of the dose at a depth of 5–15 mm with the spoiler placed in the range of 5–20 cm in front of the phantom. The normalization was made to the dose at a depth of 20 mm. Without the spoiler the dose at a 0.6 mm depth was 63%. In oblique beam incidence, the entrance doses are higher (28, 29). At a depth less than about 2 mm from the exit surface there is, apart from lack of back-scattered photons, also a lack of back-scattered electrons. The size of this effect is almost independent of field size (30) and for a 10×10 cm field and 8 MV x-rays, the dose at 0.6 mm from the exit surface is reduced by about 4% due to this effect.

In patient treatments, a blanket (0.1 g cm^{-2} thick) is wrapped around the patient to make the cast more comfortable but also to further destroy the build-down and the build-up (18).

Test measurements in Humanoid phantoms. The Table shows the basic phantom or patient input data for calculation of the AP/2 doses and the doses at 2 cm depth with the computer program at eight different levels. Figs 6 and 7 show the test of the dose-calculation method both in an R-T Humanoid adult phantom and a Pedo-RT Humanoid phantom. The solid lines are the calculated absorbed doses at points 3 cm and 1.5 cm lateral to the midline in each slice for the Humanoid and the Pedo-RT phantom respectively. The test points were placed laterally in order to eliminate the effect of the vertebra in the comparison between the calculated and measured absorbed doses, since no corrections were made for bone tissues in the calculations. No filters or boluses were used.

For the adult phantom, the absorbed doses measured are shown separately for the right and left sides of the thoracic region. The measured absorbed doses differ by more than 10% between the two sides due to lung tissue in the local beam on the right side. In other parts of the phantom, the dots represent the mean of two measurements in each slice for three irradiation occasions. In the trunk the agreement is within 2%. For the Pedo phantom the difference between the measured and calculated absorbed doses is less than 2% for most of the measurement points. In the head region of both phantoms, lower absorbed doses are measured at the levels of the skull and the mandible where thick bones interfere with the local beams.

The dosimetric parameters used in the calculation of absorbed doses in the Humanoid phantoms are based on measurements in water and plastic phantoms of rectangular shape. The test of the calculation method gives measured absorbed doses with TLD that were 1.5–2% low in

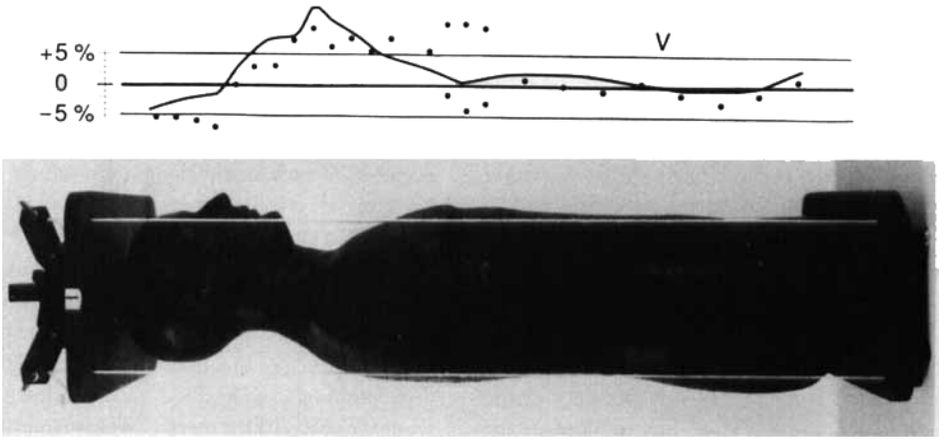

Fig. 6. Calculated (solid line) and measured (●) AP/2 absorbed doses for the adult Humanoid phantom.

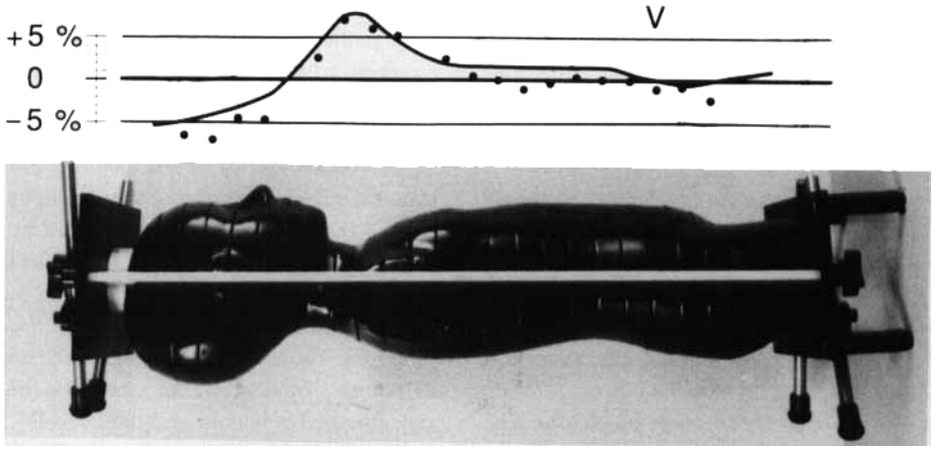

Fig. 7. Calculated (solid line) and measured (●) AP/2 absorbed doses for the Pedo Humanoid phantom.

the parts of the phantoms with homogeneous composition. Half a per cent of this difference originates from the difference in dose calibration made with TLD and the ionization chamber. Less than one per cent may depend on the elliptical shape of the phantoms. This is an estimated value from the calculation of ^{60}Co TAR for elliptical phantoms (31).

For the legs, a comparison of AP/2 doses in a cylindrical water phantom with 10 cm diameter and 30 cm long and in a phantom of rectangular shape, 13 × 15 × 10 cm, showed a difference of about 1%. Thus for 8 MV, the correction for the elliptical shape is small.

The relation between lung absorbed doses and surface doses at corresponding levels was also tested with TLD rods in polystyrene capsules (5 mm diameter) in the two Humanoid phantoms. It was found that the measured absorbed doses in the centre of the lungs were approximately the same as the absorbed doses measured at the phantom surface.

ACKNOWLEDGEMENTS

This work was supported by grants from the Kamprad Foundation Research Fund and the Lund University Hospital Donation Fund. We would like to thank Mr. Kurt Larsson for his ingenious ideas concerning the mechanics and skilful construction of many devices used in this work.

Request for reprints: Dr Gudrun Svahn-Tapper, Department of Radiation Physics, University Hospital, S-221 85 Lund, Sweden.

REFERENCES

1. Thomas ED, Buckner CD, Banaji M, et al. One hundred patients with acute leukemia treated by chemotherapy, total body irradiation, and allogeneic marrow transplantation. Blood 1977; 49: 511–33.
2. Thomas ED, Buckner CD, Clift RA, et al. Marrow transplantation for acute nonlymphoblastic leukemia in first remission. N Engl J Med 1979; 301: 597–9.
3. Keane TJ, Van Dyk J, Rider WD. Idiopathic interstitial pneumonia following bone marrow transplantation: the

relationship with total body irradiation. Int J Radiat Oncol Biol Phys 1980; 7: 1365–70.
4. Van Dyk J, Keane TJ, Kan S, Rider WD, Fryer CJH. Radiation pneumonitis following large single dose irradiation: A re-evaluation based on absolute dose to lung. Int J Radiat Oncol Biol Phys 1981; 7: 461–7.
5. Molls M, Budach V, Bamberg M. Total body irradiation: The lung as critical organ. Strahlenther Onkol 1986; 162: 226–32.
6. Meeting of Leiden, May 25–27, 1982: Journal Européen de Radiothérapie, T. 3, N° 4 1982; 157–264.
7. AAPM 17: The physical aspects of total and half body photon irradiation. AAPM Report No. 17, J. Van Dyk, chairman, 1986.
8. Glasgow GP. The dosimetry of fixed, single source hemibody and total body irradiators. Med Phys 1982; 9: 311–23.
9. Quast U. Total body irradiation—review of treatment techniques in Europe. Radiother Oncol 1987; 9: 91–106.
10. Quast U. Dosimetry of total body irradiation—a review. In: Proceedings of International Symposium on Dosimetry in Radiotherapy, IAEA-SM-298, pp. 187–210. Vienna, 1987.
11. British Journal of Radiology, Suppl No. 17: Central Axis Depth Dose Data for Use in Radiotherapy. The British Institute of Radiology, London 1983.
12. Van Dyk J. Dosimetry for total body irradiation. Radiother Oncol 1987; 9: 107–18.
13. Khan FM, Williamson JF, Sewchand W, Kim TH. Basic data for dosage calculation and compensation. Int J Radiat Oncol Biol Phys 1980; 6: 745–51.
14. Benassi M, Bianciardi L, D'Angelo L, Guerra AS, Lovisolo GA, Arcangeli G. Dosimetric problems in total body irradiation. In: Proceedings of International Symposium on Dosimetry in Radiotherapy, IAEA-SM-298, pp. 221–230, Vienna, 1987.
15. Khan FM, Gerbi BJ, Deibel FC. Dosimetry of asymmetric x-ray collimators. Med Phys 1986; 13: 936–41.
16. Mohan R, Chui C. Energy and angular distributions of photons from medical linear accelerators. Med Phys 1985; 12: 592–7.
17. Nilsson P, Svahn-Tapper G. A method for estimating off-axis photon beam quality for high energy accelerators. In: Abstract book of the 6th Annual Meeting of the European Society for Therapeutic Radiology and Oncology, p. 416, Lisboa, Portugal 1987.
18. Findley DO, Skov DD, Blume GK. Total body irradiation with a 10 MV linear accelerator in conjunction with bone marrow transplantation. Int J Radiat Oncol Biol Phys 1980; 6: 695–702.
19. Podgorsak EB, Pla C, Evans MDC, Pla M. The influence of phantom size on output, peak scatter factor, and percentage depth dose in large-field photon irradiation. Med Phys 1985; 12: 639–45.
20. Van Dyk J, Leung PMK, Cunningham JR. Dosimetric considerations of very large cobalt-60 fields. Int J Radiat Oncol Biol Phys 1980; 6: 753–9.
21. Goede MR, Anderson DW, McCray KL. Corrections to megavoltage depth-dose values due to reduced backscatter thickness. Med Phys 1977; 4: 123–6.
22. Aget H. Dosimetry of total body irradiation. J Eur Radiother 1982; 3: 183–9.
23. International Electrotechnical Commission IEC Standard, Publication 731: Medical electrical equipment: Dosimeters with ionization chambers as used in radiotherapy. Bureau Central de la Commission Electrotechnique Internationale, Geneva, 1982.
24. Christ G. In-vivo dosimetry for TBI. Strahlenther Onkol 1987; 163: 220–1.
25. Spokas J, Meeker RD. Investigation of cables for ionization chambers. Med Phys 1980; 7: 135–40.
26. ICRU 21. Radiation Dosimetry: Electrons with initial energies between 1 and 50 MeV. International Commission on Radiation Units and Measurements, Report No. 21, Washington DC, USA 1972.
27. Cunningham JR, Woo M, Rogers DWO, Bielajew AF. The dependence of mass energy absorption coefficient ratios on beam size and depth in a phantom. Med Phys 1986; 13: 496–502.
28. Gagnon WF. Physical factors affecting absorbed dose to the skin from cobalt-60 gamma rays and 25-MV x-rays. Med Phys 1979; 6: 285–90.
29. Ssengabi J. Studies of photon beam properties in therapeutic applications. (PhD Thesis) Stockholm: University of Stockholm, 1978.
30. Lambert GD, Liversage WE, Hirst AM, Doughty D. Exit dose studies in megavoltage photon therapy. Br J Radiol 1983; 56: 329–34.
31. Jayaraman S, Agarwal SK, Bhaduri D. Influence of surface shape on tissue-air ratio for cobalt-60. Med Phys 1981; 8: 459–61.